Hydrogen Decrepitation Behaviors of Novel RE–Fe–B Strip-Casting Alloys Based on Misch Metal

Yanli Liu[1,2,3], Jianjun Zhou[1], Xin Wang[1], Fei Liu[1], Qiang Ma[1,2], Tongyun Zhao[2], Fengxia Hu[2], Jirong Sun[2], and Baogen Shen[2]

[1]School of Science, Inner Mongolia University of Science and Technology, Baotou 014010, China
[2]State Key Laboratory of Magnetism, Institute of Physics, Chinese Academy of Sciences, Beijing 100190, China
[3]University of Chinese Academy of Sciences, Beijing 100049, China

To reduce the Nd–Fe–B material cost and balance the utilization of rare earth sources, the misch metal (MM) substitution for Nd in the sintered magnet attracts interest. Under the processing of fabricating Nd–Fe–B magnet, hydrogen decrepitation (HD) is widely used to obtain magnetic powder; however, the HD behaviors of RE–Fe–B strips based on MM may be complex. The HD behaviors of the $[(Pr, Nd)_{1-x}MM_x]_{30.8}Fe_{bal}Co_{1.4}$ $B_{0.97}$ ($x = 0-1$) strips were studied under 0.2 MPa pressure. We find that it is similar to the Nd–Fe–B, 2:14:1 tetragonal structure of RE–Fe–B strips based on MM which is not broken during hydrogen decrepitating. But the $REFe_2$ phase in $MM_{30.8}Fe_{bal}Co_{1.4}B_{0.97}$ disappears dramatically as a result of hydrogenation. For the samples with MM, the HD process is quicker and the particle size gets smaller than that for free MM, especially for samples with 35 wt.% MM, which may be attributed to La and Ce elements.

Index Terms— **Hydrogen decrepitation (HD), misch metal (MM), $REFe_2$ phase, surface activation.**

I. Introduction

DUE to the excellent magnetic properties, the demands of Nd–Fe–B magnets are increasing and the use of closely relied rare earth (RE) Pr/Nd/Dy/Tb is expanding [1], [2]. In this regard, there exists serious contradiction between the increasing demand for Nd–Fe–B and the tight supply of raw materials. Hence, high abundance and low-cost La/Ce substitution for Nd to fabricate RE–Fe–B magnets has become a research focus [3]–[8]. However, from misch REs to pure La/Ce/Pr/Nd metal, the extraction and purifying processes are very complex and influence ecological environment. Based on protecting the environment and balanced use of RE resource, the predecessor misch metal (MM), which contains La, Ce, Pr, and Nd elements with natural ratio (26–29 wt.% La, 49–53 wt. % Ce, 4–6 wt.% Pr, and 15–17 wt.% Nd) [9], is directly applied to prepare RE–Fe–B magnets. According to the literatures, RE–Fe–B magnets with MM substitution have preferable magnetic performances, although the intrinsic magnetic properties of $MM_2Fe_{14}B$ are inferior to $Nd_2Fe_{14}B$, yet the magnetic energy product of the isotropic $MM_{13}Fe_{81}B_6$ melting ribbons have reached 12 MGOe [10]. The magnetic properties of the sintered RE–Fe–B with 30.3 at.% MM substitution are $H_{cj} = 7.11$ kOe and $(BH)_{max} = 41$ MGOe, which is the highest in magnets with the same composition prepared by all kinds of approaches. In a word, powder metallurgy to fabricate sintered RE–Fe–B magnets with MM is an effective approach to realize quantitative production.

Generally, the powder metallurgy method to fabricate sintered Nd–Fe–B magnets is composed of strip-casting, hydrogen decrepitation (HD), jet milling, aligning under magnetic field, sintering, and annealing. Among the process, HD is the key process. Under hydrogen atmosphere (or elevated pressure), due to the hydrogen absorption of $Nd_2Fe_{14}B$ and Nd-rich phase, the induced crystal volume expanding and subsequent stresses make the material crushed and pulverized. The obtained coarse powders are friable and easy to be milled than the conventional powders. The HD process has been demonstrated to have a great influence on the powder size and shape and the microstructure of the final magnets [11], [12]. For the RE–Fe–B strips with the La/Ce substitution, it is more difficult to be hydrogenated than the Nd–Fe–B strips, which is ascribed to higher oxygen affinity of La and Ce than Nd [13]. But La and Ce are considered that there are better the properties of hydrogen absorption than Pr and Nd based on thermodynamic simulation and are the typical hydrogen storage material [14]. There are the two diametrically opposed views. In addition, due to the phase constitution and microstructure of (Nd, MM)–Fe–B strips is different from Nd–Fe–B, the HD behavior of these strips may be also different. Hence, to further improve the magnetic properties and stimulate quantity production, it is necessary to study the HD behaviors of the RE–Fe–B strips based on MM.

II. Experiment

The alloy flakes with the nominal composition of $[(Pr, Nd)_{1-x}MM_x]_{30.8}Fe_{bal}Co_{1.4}B_{0.97}$ (wt.%, $x = 0, 0.35, 0.50, 1.00$) were prepared by induction melting and strip-casting with a copper wheel speed of 1.5 m/s. The mean thickness of the obtained strips was about 0.3 mm. In the experiment, MM is

Manuscript received March 18, 2020; revised June 16, 2020; accepted August 29, 2020. Date of publication September 22, 2020; date of current version November 18, 2020. Corresponding author: B. Shen (e-mail: shenbg@iphy.ac.cn).

Color versions of one or more of the figures in this article are available online at https://ieeexplore.ieee.org.

Digital Object Identifier 10.1109/TMAG.2020.3025208

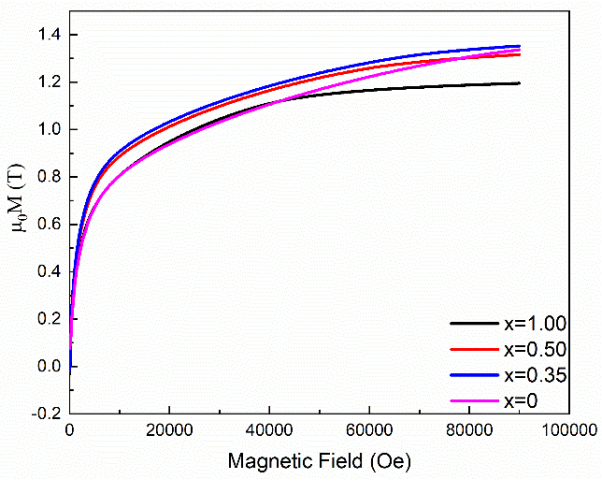

Fig. 1. Initial magnetization curves of the $[(Pr, Nd)_{1-x}MM_x]_{30.8}Fe_{bal}Co_{1.4}B_{0.97}$ ($x = 0$, 0.35, 0.50, and 1) strips at 300 K.

one of the typical MM from Bayan Obo mine in Baotou, which contains about La 28.63 wt.%, Ce 50.13 wt.%, Pr 4.81 wt.%, Nd 16.28 wt.%, and <1 wt.% others.

The HD process for $[(Pr, Nd)_{1-x}MM_x]_{30.8}Fe_{bal}Co_{1.4}B_{0.97}$ ($x = 0$, 0.35, 0.50, 1.00) strips was separately performed in a high-pressure autoclave with initial hydrogen pressure of 0.2 MPa (the value of the hydrogen pressure is generally applied in industrial manufacture) at 293 K. The mass of the strips loaded in the autoclave was 1000 g every time. During the whole process, the pressure was detected by the pressure sensor and the temperature was monitored by the thermocouple in the autoclave. The autoclave was charged with hydrogen automatically as soon as the pressure dropped to 0.168 MPa. The hydrogen content of the samples was tested by Oxygen Nitrogen Hydrogen analyzer (Eltra ONH-2000). The phase constitution was analyzed by X-ray diffraction (Panalytical X'pert Powder system) with Co Ka radiation. The micro-structure was observed by a scanning electron microscope (Phenom Prox) with an energy-dispersive X-ray spectrometer (EDS). Subsequently, the magnetization field *(M-H)* curves of the strips were also measured at 300 K by a Quantum Design PPMS with a maximum field of 9 T. The particle distribution of the powder after the HD process was tested by the laser particle diameter analyzer (SYMPATEC HELOS&RODOS/L type).

III. Results and Discussion

Fig. 1 shows the initial magnetization curves of $[(Pr, Nd)_{1-x}MM_x]_{30.8}Fe_{bal}Co_{1.4}B_{0.97}$ ($x = 0$, 0.35, 0.50, 1) strips at 300 K. According to the law of approach to saturation, the saturation magnetization $\mu_0 M_s$ is obtained and summarized in Table I. With increasing MM substitution, the value of $\mu_0 M_s$ gradually declines. But these values are higher than that of ferrites. The RE–Fe–B sintered magnets with MM substitution could plug the gap between Nd–Fe–B magnets and ferrites. However, the magnetic performances of the RE–Fe–B sintered magnets are influenced by the HD process [10], [16]. Therefore, the study on the HD behavior of $[(Pr, Nd)_{1-x}MM_x]_{30.8}Fe_{bal}Co_{1.4}B_{0.97}$ strips is very necessary to realize mass production.

TABLE I

$\mu_0 M_s$ VALUE OF $[(PrNd)_{1-x}MM_x]_{30.8}Fe_{bal}Co_{1.4}B_{0.97}$ ($x = 0$, 0.35, 0.50 AND 1) STRIPS, THE OXYGEN, HYDROGEN CONTENT BEFORE AND AFTER HD PROCESS, AND THE VOLUME VARIATION AFTER HD PROCESS

x=	0	0.35	0.50	1.00
$\mu_0 M_s$ (T)	1.57	1.50	1.44	1.26
Oxygen(ppm) bef. HD	84.95	87.57	79.30	84.61
Oxygen(ppm) aft. HD	897.2	1098	1169	1110
Hydrogen(ppm) aft. HD	4663	4885	4795	4771
ΔV/V (%) aft. HD	2.42	2.62	2.00	2.40

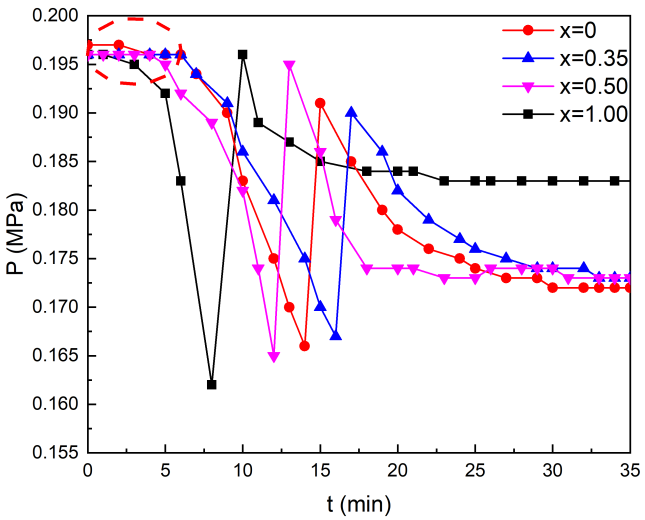

Fig. 2. Hydrogen decrepitation curves of the $[(Pr, Nd)_{1-x}MM_x]_{30.8}Fe_{bal}Co_{1.4}B_{0.97}$ ($x = 0$, 0.35, 0.50, and 1) strips with initial hydrogen pressure of 0.2 MPa at 293 K.

Fig. 2 illustrates the HD behaviors of the $[(Pr, Nd)_{1-x}MM_x]_{30.8}Fe_{bal}Co_{1.4}B_{0.97}$ ($x = 0,0.35,0.50,1$) strips. The hydrogen pressure P versus time t plots are presented by exposing the strips to pure hydrogen atmosphere with hydrogen pressure of 0.2 MPa. In general, the HD process is composed of sample surface activation, hydrogenation of the RE-rich phase, and hydrogen absorption of the $RE_2Fe_{14}B$ phase [17]. With increasing MM substitution for Pr–Nd alloy, the duration of the sample surface activation decreases gradually (the region circled by the red line in Fig. 2), and the speed of hydrogen absorption also increases which is demonstrated by the slopes of the curves in Fig. 2. The phenomenon is entirely different from that of RE–Fe–B with other RE element substitution except for the La and Ce elements [18]. For these strips with increasing MM content, the amount of La and Ce in the RE-rich phase and $RE_2Fe_{14}B$ phase also increases gradually, as is found in [15]. Due to the active reaction between La/Ce and H [14], the duration of surface activation and the speed of hydrogen absorption may be affected by the La and Ce content of the RE-rich phase for the $[(Pr, Nd)_{1-x}MM_x]_{30.8}Fe_{bal}Co_{1.4}B_{0.97}$ strips, based on the similar thickness, surface roughness, and oxygen content factors (the process is the same in the strip-casting procedure, and the content of oxygen is similar, as is shown in Table I). As is shown in Fig. 2, the durations of the whole HD process of

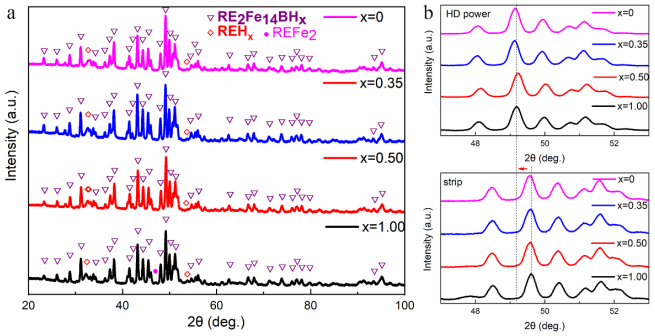

Fig. 3. X-ray diffraction patterns of the $[(Pr, Nd)_{1-x}MM_x]_{30.8}Fe_{bal}Co_{1.4}B_{0.97}$ ($x = 0$, 0.35, 0.50, and 1) strips (a) after the HD process and (b) enlarged X-ray diffraction patterns of 2θ between 47° and 53° of the $((PrNd)_{1-x}MM_x)_{30.8}Fe_{bal}Co_{1.4}B_{0.97}$ strips before and after the HD process.

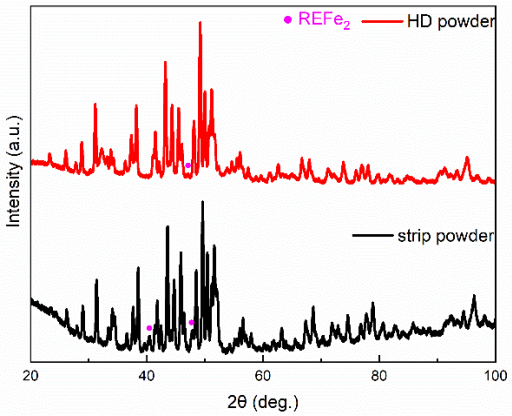

Fig. 4. X-ray diffraction patterns of the $MM_{30.8}Fe_{bal}Co_{1.4}B_{0.97}$ strips before and after the HD process.

$[(Pr, Nd)_{1-x}MM_x]_{30.8}Fe_{bal}Co_{1.4}B_{0.97}$ strips ($x = 0.35 - 1$) with MM get shorter than that of the $(PrNd)_{30.8}Fe_{bal}Co_{1.4}B_{0.97}$ strips, which is beneficial to industrial production.

Fig. 3(a) shows the XRD profiles of $[(PrNd)_{1-x}MM_x]_{30.8}Fe_{bal}Co_{1.4}B_{0.97}$ ($x = 0 - 1$) powder after the HD process. A series of characteristic diffraction peaks corresponding to the $RE_2Fe_{14}BH_x$ phase (space group P42/mnm) are similar to that of the $RE_2Fe_{14}B$ phase. It is implied that the 2:14:1 tetragonal phase in all the samples with different MM ($x = 0 - 1$) can keep stable in the HD process. But the characteristic peaks corresponding to the $RE_2Fe_{14}BH_x$ phase shift toward the left relative to that of the $RE_2Fe_{14}B$ phase, as is shown in Fig. 3(b). The movement distance of the peak position is 0.419° for $x = 0$, 0.454° for $x = 0.35$, 0.349° for $x = 0.50$, and 0.416° for $x = 1$, respectively. Based on the angle of 2:14:1 tetragonal phase diffraction peak before and after the HD process [17], the relative variation in the lattice volume($\Delta V/V$) is calculated and displayed in Table I. The variation tendency of $\Delta V/V$ with MM content accords with the results of hydrogen content in Table I tested by the Oxygen Nitrogen Hydrogen analyzer. The hydrogen absorption content of the $RE_2Fe_{14}B$ phase in the $[(Pr, Nd)_{1-x}MM_x]_{30.8}Fe_{bal}Co_{1.4}B_{0.97}$ ($x = 0 - 1$) strips is in the range of 4000–5000 ppm, as is reported in [19] and [20]. After the HD process, the amount of hydrogen in $[(Pr, Nd)_{1-x}MM_x]_{30.8}Fe_{bal}Co_{1.4}B_{0.97}$ powder increases with the increasing MM. But for $x = 0.35$, the hydrogen content is highest, which may be attributed to the larger lattice constants of $RE_2Fe_{14}B$ with 35 wt.% MM than that of $Nd_2Fe_{14}B$. In addition, before the HD process, for $x = 1$, there exists the $REFe_2$ phase that is verified as a result of the appearance of diffraction peaks at $2\theta \approx 40.56°$ and $2\theta \approx 47.96°$ in Fig. 4 (the phenomenon was reported in our previous paper). But when $x = 1$ ($MM_{30.8}Fe_{bal}Co_{1.4}B_{0.97}$), the characteristic peaks of the $REFe_2$ phase disappear dramatically after the HD process. Because HD is an exothermal process, the rising temperature and hydrogen pressure could make $REFe_2$ phase hydrogen-induced amorphization and decomposition [21]–[23]. It is beneficial to fabricate high magnetic performance magnets with MM replacement ($REFe_2$ phase is paramagnetic at ambient temperature).

Fig. 5 shows the morphology of the $[(Pr, Nd)_{1-x}MM_x]_{30.8}Fe_{bal}Co_{1.4}B_{0.97}$ ($x = 0$ and 0.35) powder after the HD process.

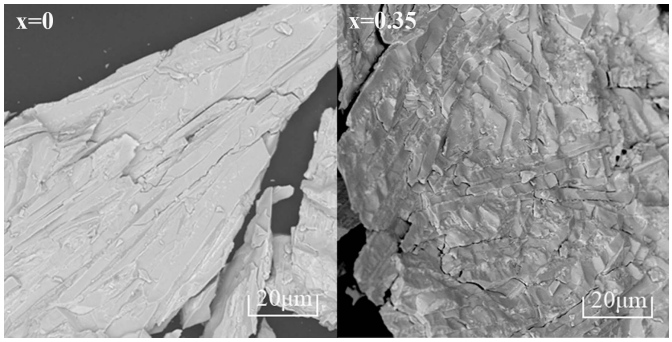

Fig. 5. SEM image of the $[(Pr, Nd)_{1-x}MM_x]_{30.8}Fe_{bal}Co_{1.4}B_{0.97}$ ($x = 0$, 0.35) powder after the HD process.

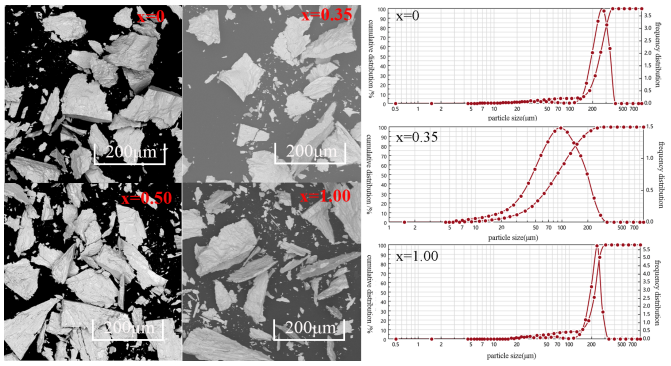

Fig. 6. Morphology and particle distribution of the $[(Pr, Nd)_{1-x}MM_x]_{30.8}Fe_{bal}Co_{1.4}B_{0.97}$ ($x = 0$, 0.35, 0.50 and 1) powder after the HD process.

Under the HD process, preferential hydrogenation of the RE-rich phase causes shear stress and brings about intracrystalline fracture eventually. The local overheating aroused by hydrogenation of the RE-rich phase makes the $RE_2Fe_{14}B$ phase hydrogenated and the volume expands, and as a result, transgranular fractures. For $x = 0.35$, as a result of more intergranular and transgranular fractures, more cracks exist and the final particle size is very smaller than that for free MM samples in Fig. 5. Eventually, as is illustrated in Fig. 6, after the HD process, the percentage of small particles for the samples with MM is higher than that for free MM samples. It makes following jet-milling easier for samples with MM.

IV. Conclusion

The HD behavior of the $[(Pr, Nd)_{1-x}MM_x]_{30.8}Fe_{bal}Co_{1.4}B_{0.97}$ ($x = 0$, 0.35, 0.50, 1) strips has been systematically investigated. During the HD process, the 2:14:1 tetragonal structure with high H_A and M_s can keep stable in all the samples ($x = 0 - 1$), but the $REFe_2$ phase disappears dramatically. Because the H atoms easily react with La/Ce, the HD process of the samples with MM is quicker than that of free MM samples, especially for the samples with 35 wt.% MM. For samples with MM, the particle size is smaller after the HD process. Therefore, quicker HD process and easier jet-milling, is beneficial to realize industrial production for Pr–Nd–MM–Fe–B magnets.

Acknowledgment

This work was supported in part by the National Key Research Program of China under Grant No. 2016YFB0700903; in part by the National Natural Foundation of China under Grant 11564030, Grant 51571126, and Grant 51590881; in part by the Fujian Institute of Innovation; in part by the Chinese Academy of Sciences under Grant FJCXY18040302; in part by the Key Program of the Chinese Academy of Sciences under Grant KJZD-EW-M05-1; and in part by the Natural Science Foundation of Inner Mongolia under Grant 2018LH05006 and Grant 2018LH05011.

References

[1] M. Sagawa, S. Fujimura, N. Togawa, H. Yamamoto, and Y. Matsuura, "New material for permanent magnets on a base of Nd and Fe (invited)," *J. Appl. Phys.*, vol. 55, no. 6, pp. 2083–2087, Mar. 1984.

[2] B.-P. Hu *et al.*, "Study of sintered Nd–Fe–B magnet with high performance of H_{cj} (kOe) + $(BH)_{max}$ (MGOe) > 75," *AIP Adv.*, vol. 3, no. 4, Apr. 2013, Art. no. 042136.

[3] O. Gutfleisch, M. A. Willard, E. Brück, C. H. Chen, S. G. Sankar, and J. P. Liu, "Magnetic materials and devices for the 21st century: Stronger, lighter, and more energy efficient," *Adv. Mater.*, vol. 23, no. 7, pp. 821–842, Feb. 2011.

[4] Z. B. Li, B. G. Shen, M. Zhang, F. X. Hu, and J. R. Sun, "Substitution of Ce for Nd in preparing $R_2Fe_{14}B$ nanocrystalline magnets," *J. Alloys Compounds*, vol. 628, pp. 325–328, Apr. 2015.

[5] J. F. Herbst, M. S. Meyer, and F. E. Pinkerton, "Magnetic hardening of $Ce_2Fe_{14}B$," *J. Appl. Phys.*, vol. 111, no. 7, Apr. 2012, Art. no. 07A718.

[6] M. G. Zhu *et al.*, "An enhanced coercivity for (CeNdPr)-Fe-B sintered magnet prepared by structure design," *IEEE Trans. Magn.*, vol. 51, no. 11, Nov. 2015, Art. no. 2104604.

[7] L. L. Zhang, Z. B. Li, Q. Ma, Y. F. Li, Q. Zhao, and X. F. Zhang, "Coercivity enhancement in (Ce,Nd)-Fe-B sintered magnets prepared by adding NdHx powders," *J. Magn. Magn. Mater.*, vol. 435, pp. 96–99, Aug. 2017.

[8] J. Jin, Z. Wang, G. Bai, B. Peng, Y. Liu, and M. Yan, "Microstructure and magnetic properties of core-shell Nd-La-Fe-B sintered magnets," *J. Alloys Compounds*, vol. 749, pp. 580–585, Jun. 2018.

[9] M. Zhang, Z. Li, B. Shen, F. Hu, and J. Sun, "Permanent magnetic properties of rapidly quenched $(La,Ce)_2Fe_{14}B$ nanomaterials based on La–Ce mischmetal," *J. Alloys Compounds*, vol. 651, pp. 144–148, Dec. 2015.

[10] W.-L. Zuo *et al.*, "High performance misch-metal (MM)-Fe-B magnets prepared by melt spinning," *J. Alloys Compounds*, vol. 695, pp. 1786–1792, Feb. 2017.

[11] I. I. Bulyk *et al.*, "Features of the HDDR process in R–Fe–B ferromagnetic alloys (R is a mixture of Nd, Pr, Ce, La, Dy and others)," *J. Alloys Compounds*, vol. 370, nos. 1–2, pp. 261–270, May 2004.

[12] M. Yan, L. Q. Yu, J. M. Wu, and X. G. Cui, "Improved magnetic properties and fracture strength of NdFeB by dehydrogenation," *J. Magn. Magn. Mater.*, vol. 306, no. 2, pp. 176–180, Nov. 2006.

[13] J. Jin *et al.*, "Novel hydrogen decrepitation behaviors of (La, Ce)-Fe-B strips," *AIP Adv.*, vol. 8, no. 5, May 2018, Art. no. 056233.

[14] W. Luo, X. H Zeng, A. D. Xie and T. Y. Yu, "The thermodynamic computational model and its application for rare earth hydrogenation reaction," *Model. Simul.*, vol. 4, no. 1, pp. 33–39, 2015.

[15] X. Yu *et al.*, "Intrinsic evolution of novel $(Nd, MM)_2Fe_{14}B$-system magnetic flakes," *Appl. Phys. A, Solids Surf.*, vol. 124, no. 1, p. 15, Jan. 2018.

[16] R. Li *et al.*, "Magnetic properties of (misch metal, Nd)-Fe-B melt-spun magnets," *AIP Adv.*, vol. 7, no. 5, May 2017, Art. no. 056207.

[17] X. T. Li *et al.*, "Effect of hydrogen pressure on hydrogen absorption of waste Nd–Fe–B sintered magnets," *J. Magn. Magn. Mater.*, vol. 473, pp. 144–147, Mar. 2019.

[18] B. Saje, J. Holc, and S. Beseničar, "Hydrogenation process of Nd-Dy-Fe-B alloy," *J. Mater. Sci.*, vol. 27, no. 10, pp. 2682–2686, May 1992.

[19] R. Bezdushnyi, R. Damianova, I. S. Tereshina, N. Y. Pankratov, and S. A. Nikitin, "Hydrogen absorption and its effect on magnetic properties of $Nd_2Fe_{14}B$," *J. Magn. Magn. Mater.*, vol. 453, pp. 226–230, May 2018.

[20] M. A. R. Önal *et al.*, "Comparative oxidation behavior of Nd–Fe–B magnets for potential recycling methods: Effect of hydrogenation pretreatment and magnet composition," *J. Alloys Compounds*, vol. 728, pp. 727–738, Dec. 2017.

[21] K. Aoki, M. Dilixiati, and K. Ishikawa, "Hydrogen-induced transformations in C15 laves phases $CeFe_2$ and $TbFe_2$ studied by pressure calorimetry up to 5 MPa," *J. Alloys Compounds*, vols. 356–357, pp. 664–668, Aug. 2003.

[22] K. Aoki, H.-W. Li, M. Dilixiati, and K. Ishikawa, "Formation of crystalline and amorphous hydrides by hydrogenation of C15 laves phase YFe_2," *Mater. Sci. Eng., A*, vols. 449–451, pp. 2–6, Mar. 2007.

[23] K. Aoki, H.-W. Li, and K. Ishikawa, "Process and mechanism of hydrogen-induced amorphization in C15 laves phases RFe_2," *J. Alloys Compounds*, vols. 404–406, pp. 559–564, Dec. 2005.